ANSTO/E-766

FLOW ASSURANCE IN A MODEL CRUDE OIL: A STRUCTURAL AND RHEOMETRIC STUDY

E. Drabarek [+], C. Muzny [§], G. Bryant [#], and H. J. M. Hanley [+ * #]

June 2008

ISBN: 1921268050

[+] **Australian Nuclear Science and Technology Organization, PMB 1, Menai NSW 2234.**

[§] **Division 838, National Institute of Standards and Technology, 325 Broadway, Boulder, 80305, CO, USA.**

 # Applied Physics, School of Applied Sciences, RMIT University, GPO Box 2476V, Melbourne, 3001

[*] **Research School of Chemistry, Australian National University, Canberra, ACT 0200.**

Abstract

This report investigates how the technique of small angle neutron scattering (SANS) helps elucidate the phenomenon of wax deposition in a petroleum crude oil. Specifically, we report SANS data, supplemented by results from dynamic light scattering (DLS), obtained from a synthetic petroleum crude oil: a mixture of commercial paraffin wax dissolved in an octane/cyclohexane solvent. The system is a gel below the cloud point. The onset and growth of this waxy gel, and changes in its nanostructure, are recorded here as a function of temperature over the range $10 \leq T/°C \leq 65$.

SANS indicates that the wax has a definite characteristic length of about 100 Å (10 nm) which can be observed at temperatures as high as 57°C, but DLS indicates that the wax also contains very large structures - of the order of a micrometer - over the temperature range 30° - 50°C.

The structural studies are supplemented by corresponding sets of viscosity and stress data taken from the gelling wax when subjected to an applied shear. We observe that the stress will increase as the temperature falls - i.e. as the system gels - but, in general, will then reach a maximum and tend to decline.

The wax results are compared with those from a similar system in which the wax is replaced by n-docosane (C_{22}), one of the major components of the wax. Significant differences between the behavior of the wax and the pure component in the solvents are noted. The SANS patterns to 20°C from docosane do not give any indication of the nanoscale structure observed from the wax; the DLS patterns for docosane indicate that a solidification occurs over a very narrow temperature range between 10°C and 12°C, accompanied by a dramatic slowing of the dynamics; the large scale structure seen in the wax mixtures is not evident; and the rheological behavior of the two systems is markedly different.

The paper also compares and contrasts the rheological behavior of the wax gel with that observed from a defined system, gelled colloidal silica. Strong similarities are apparent.

1.0 Introduction: Flow assurance and deposition

1.1 Flow assurance

Flow assurance: as the name implies, crude oil has to flow smoothly from the reservoir to the refinery. Flow, however, is potentially severely hindered by deposition, scaling, aggregation and gelation (Figure 1) that can occur when the operating conditions vary: for example, when the crude is subjected to substantial temperature changes as it is pumped from the reservoir to storage, when fluids are introduced into the reservoir for enhanced oil recovery, or when crudes from different reservoirs are mixed. In the worst-case scenario, the well and/or the transmission pipelines could become completely blocked. Even if this did not happen, a routine control of the flow requires expensive corrective practices: installing larger diameter pipes, increasing pumping pressures, maintaining higher temperatures, diluting the crude with solvents, and so on [1]. This, of course, is known and the economic motivation for research into flow assurance is well established and acknowledged across the petroleum industry [2].

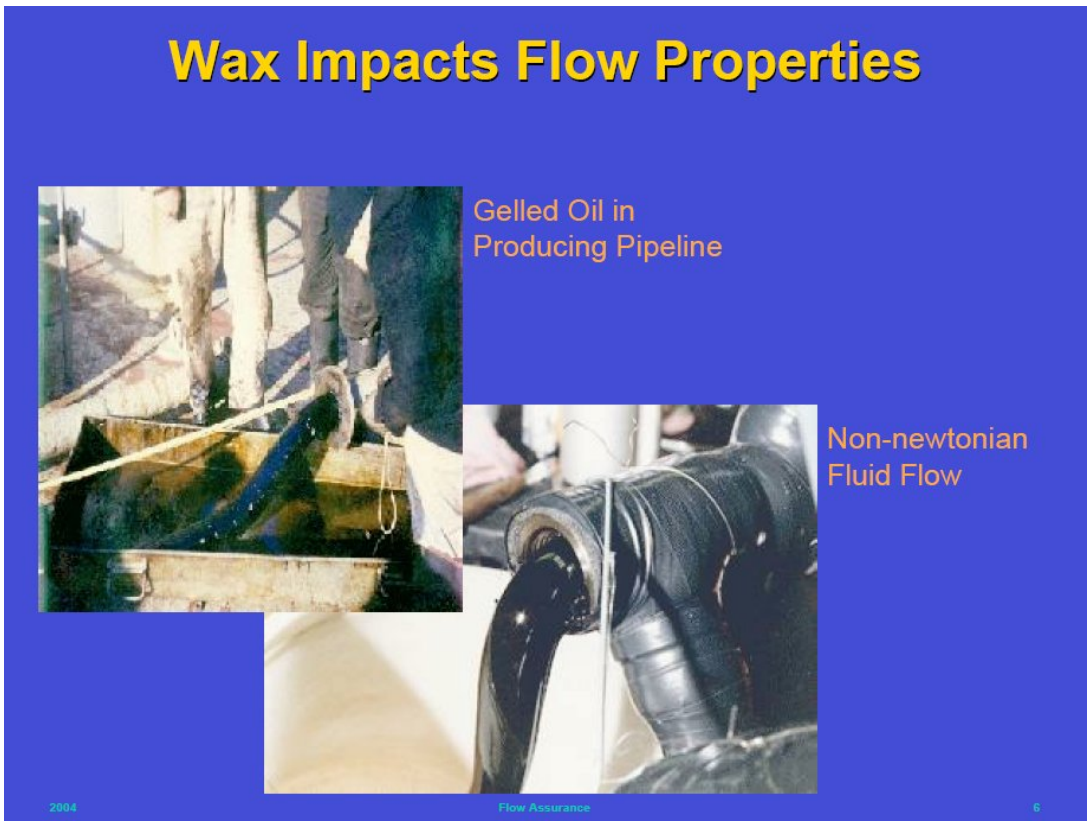

Figure 1. Gelled oil in a pipeline. An illustration of how normally free flowing petroleum liquid can appear if the operating conditions promote waxy gelation. Clearly flow would not be assured should this occur. Figure provided by Dr. Bob Hurle, University of Western Australia and used with permission.

1.2 Petroleum deposits

Conventionally, most petroleum deposits are classified as hydrates, asphaltenes or waxes.

Hydrates are gases entrapped in a fluid cage in the form of crystals but are less likely to cause transmission problems. Of more relevance are asphaltenes and, of special interest

here, wax. In general, asphaltenes are complex micellar/colloidal suspensions that precipitate from a dispersion, and waxes are heavy paraffinic solids that precipitate out of a liquid solution to form a gel. Asphaltenes can deposit at any point along the flow path, they can plug the pores of the oil-bearing rock, and they can deposit on valves, pipes, and tanks or on any surface. Waxes are gels that form in the transmission pipelines.

The reasons deposition can occur are complex and varied, especially because the mechanisms are inter-related [3] and are themselves influenced by impurities – including water – in the crude oil. Simplistically, however, asphaltene precipitation is a flocculation of suspended particles, while wax formation is a liquid-solid phase transition from a liquid mixture. As a flocculation process, asphaltene formation will be sensitive to the nature of the medium – pH, ion content, chemical content and the like; conversely, as a liquid-solid transition, wax formation will be especially, but not exclusively, sensitive to a drop in temperature.

1.3 Phase diagram and a crude oil flow path

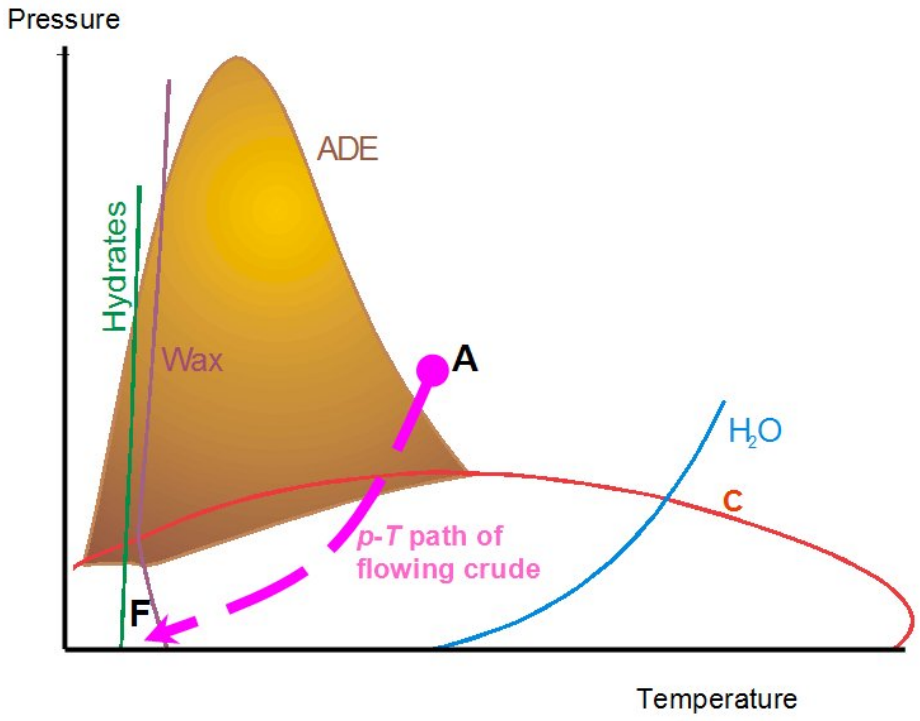

Figure 2. A schematic 'phase diagram' of a crude oil system. Shown are the asphaltene deposition envelope (ADE) in *p*-*T* space, a wax formation line, a hydrate formation line, a typical dew-bubble point envelope (with critical point C) and the vapor pressure curve for water. This diagram is typical for a petroleum fluid, but the details can vary substantially. Figure provided by Dr. Bob Hurle, University of Western Australia and used with permission.

Figure 2 displays a schematic pressure (*p*) - temperature (*T*) 'phase diagram' for typical petroleum system. Shown are the asphaltene deposition envelope (ADE – the region in *p*-*T* space in which asphaltene deposition occurs), a wax formation line (the temperature below which wax deposition is to be expected), a hydrate formation line, a typical dew-bubble point envelope, and the vapor pressure curve for water. As crude oil flows from the reservoir to the refinery, it tracks a typical *p*-*T* path indicated in the figure.

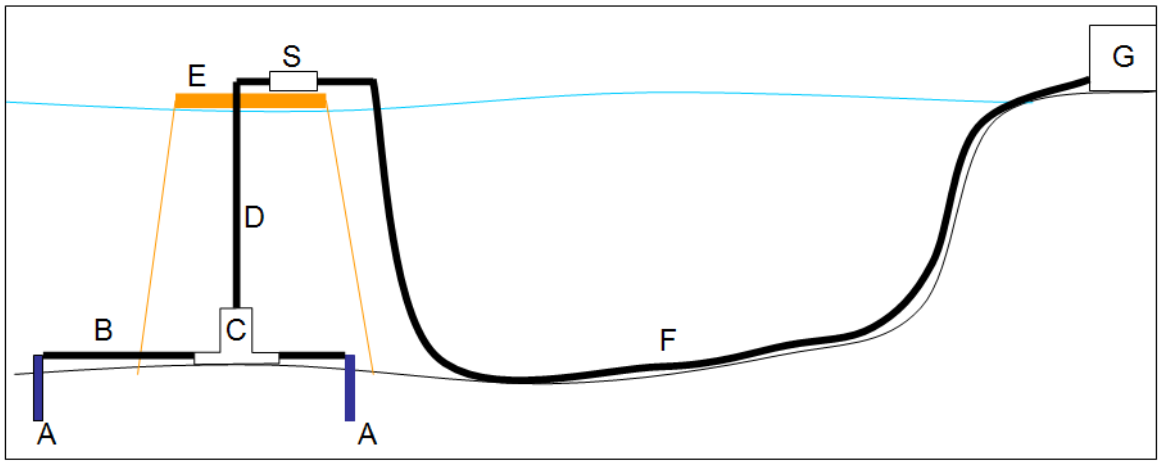

Figure 3. A path of the petroleum liquid from an offshore reservoir to the refinery. In this schematic diagram we have drawn two wells, A, connected by pipelines B to a manifold on the seabed, C, which, in turn, is connected by pipeline D to the platform separator, E. After some processing, the crude flows through pipe F to an onshore separator, G. As we point out in the text, the features of this diagram, number of wells, length of pipelines, etc. can vary substantially; as can the temperature and pressures of the several environments.

A schematic of a reservoir-refinery network is represented by Figure 3. Shown is a flow of crude produced offshore to a process plant onshore. To make our point we consider two wells (A) linked by pipelines (B) to a manifold (C) on the seabed, which is connected by pipe (D) to the separator (E) on the platform.

If the reservoir is about 3300 feet (1 km) below the seabed, the crude at reservoir conditions will be a mixture of liquid hydrocarbons, water and, possibly, gas at a typical temperature of 300°F (150°C) at a pressure of 3000 psi (20 MPa). At platform conditions, however, the temperature and pressure of the produced stream will have decreased to about 150°F (75°C) or less, and to about 600 psi (4 MPa). Most of the water, some impurities, and a portion of the gas are removed by the platform separator (S). The resulting crude stream is now piped (F) to an onshore process facility (G). During this passage, its pressure will become of the order of 150 psi (1 MPa) and the sea will moderate its temperature.

Referring to Figure 2: the p-T path of this particular process would initiate at or near the ADE region, then trace below it as the operating temperature and pressure decline. The path would intersect the wax formation line as the pressure and temperature drop further. Thus - in this example - asphaltene deposition would be likely near the reservoir but would not be expected at the operating conditions above the seabed. Wax formation, however, most likely would take place in pipeline (F).

Figure 3, and the sample operating conditions are of course only representative. For example, a large field may require two or three offshore production platforms with as many as 30 wells to each platform. Each well could be drilled to over 10000 feet (3000 m) below the seabed and, at this depth, reservoir temperatures and pressures are of the order of 250°F (115°C) and 5000 psi (35 MPa), respectively. Since the temperature in a well bore decreases by 30°C per kilometer below the surface, and since the pressure falls with height, the temperature and pressure of the crude will fall substantially by the time it has flowed to the platform. Moreover, the horizontal seabed pipes (B) could stretch for a hundred kilometers or more.

In short, any number of p-T paths could be superimposed on Figure 2. Furthermore, the locations of the phase boundaries are also schematic, since they depend on the

composition of the particular crude in question. Deposition - most likely asphaltene formation - might also occur if crudes from different wells are mixed: in this simple example, mixing might occur at the seabed manifold (C), or at the platform (E), or even at the onshore separator (G) if the separator is handling crudes from more than one source.

2.0 Objective: shear influenced wax deposition

The objective of this work is to understand wax deposition better by investigating its possible structure on the micro- and nanoscales. In this first attempt we investigate structure by small angle neutron scattering (SANS) and by dynamic light scattering (DLS). These studies are coupled with a comprehensive investigation of the shear induced rheological behavior of the system.

At this point two remarks are relevant, namely:

(1) The distinction between flocculation and gelation should be noted. Flocculation is characterized by the formation of particulate clusters with a density different from the initial sol. A floc will, therefore, separate from the solvent through gravitational settling or centrifugation. Gelation is the growth of a continuous network of clusters which will eventually span the system's container, and the macroscopic density is identical to that of the initial suspension, Furthermore, in contrast to a system that flocs, a gel has a divergent viscosity and behaves as an elastic solid, even though it is structurally bicontinuous, having a skeleton which is penetrated completely by the solvent. In this context, precipitation of heavy hydrocarbons and/or aromatics present in the crude is a flocculation and wax deposition is a gelation.

(2) We hypothesize that the properties and behavior of a gelling system are fundamentally influenced by the action of flow (that is, by an applied shear or stress) so that the thermodynamic stability criteria are shear rate dependent. Thus, in principle, the location of the ADE and the wax formation line in Figure 2 will be a defined function of the flow rate [4], as would the applied shear rate - stress relation [5, 6].

Hence, if the mechanism behind a typical deposition scenario, for example that illustrated by Figure 4, is to be understood it helps to recognize that wax is indeed a gel and that the formation and break-up of the gel is a statistical mechanical phenomenon with the shear rate as a defined input variable. We adopt this viewpoint in this work. In fact, the work discussed here follows the pattern of our treatment of a defined and largely understood system, namely colloidal silica [7, 8]. [Significant overlaps in the behavior of gelling silica and wax formation are discussed further in the Appendix.]

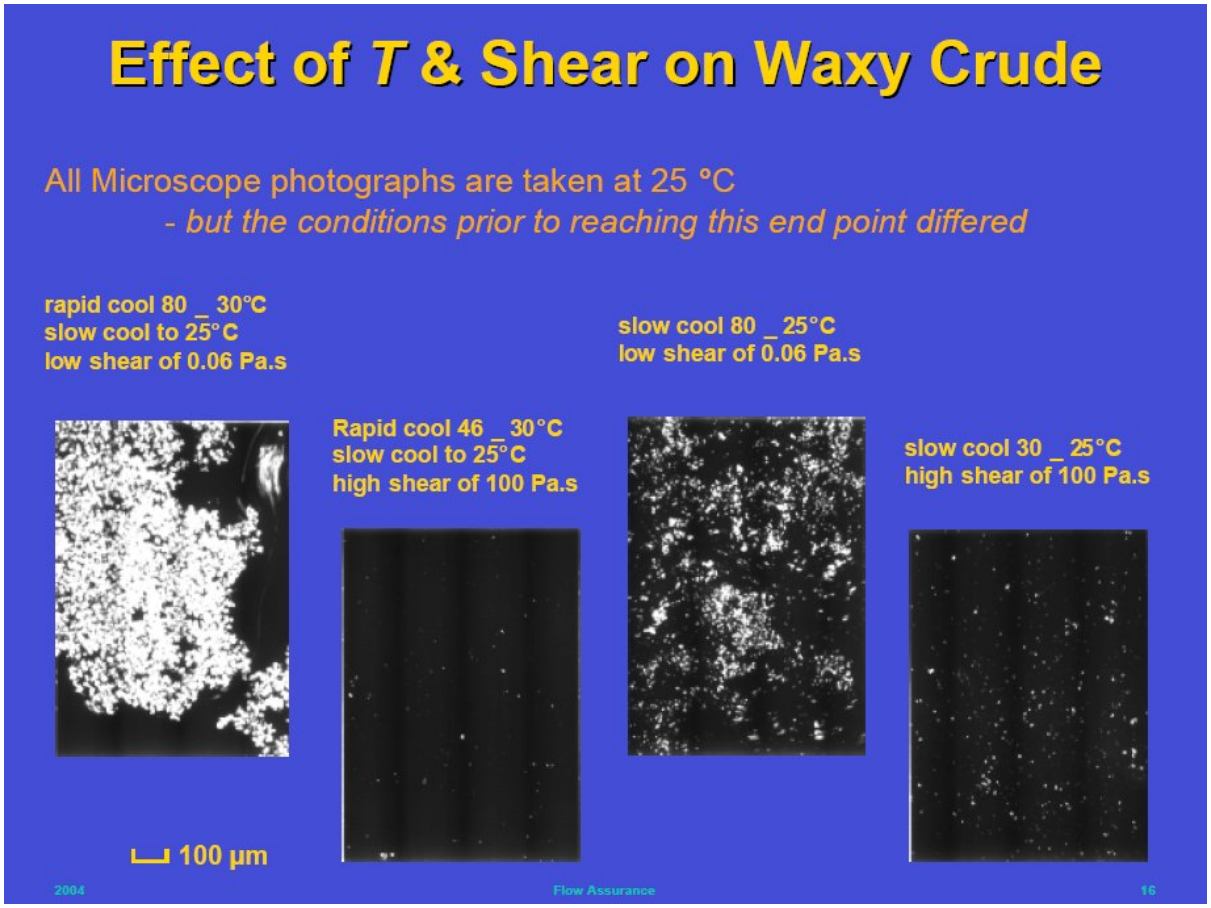

Figure 4. Effect of shear on waxy crudes. The extent of gelation depends on the rate of cooling to the cloud point, but it is noticeable that the amount of precipitation, and hence the amount of gel formation, is strongly retarded by the action of the high shear. Figure provided by Dr. Bob Hurle, University of Western Australia and used with permission.

3.0 Samples, and sample preparation

Working with a real waxy crude oil is deferred for future work. Here the experiments were carried out on model crude made up of a commercial paraffin wax mixed with a 50/50 cyclohexane/octane solvent [9]. In addition, we studied a system of the heavy hydrocarbon n-docosane, C_{22}, mixed into the same solvent – so selected in order to observe differences between the deposition from the multicomponent hydrocarbon wax and from a single species. Docosane was the pure hydrocarbon of choice because a chromatographic analysis [10], Figure 5, indicates that it makes up a significant hydrocarbon fraction in the wax. (Docosane is also a typical component in many samples of crude oil worldwide [11].) For a given mixture, results from all the experiments - SANS, DLS and the rheometric studies - were reported as a function of decreasing temperature.

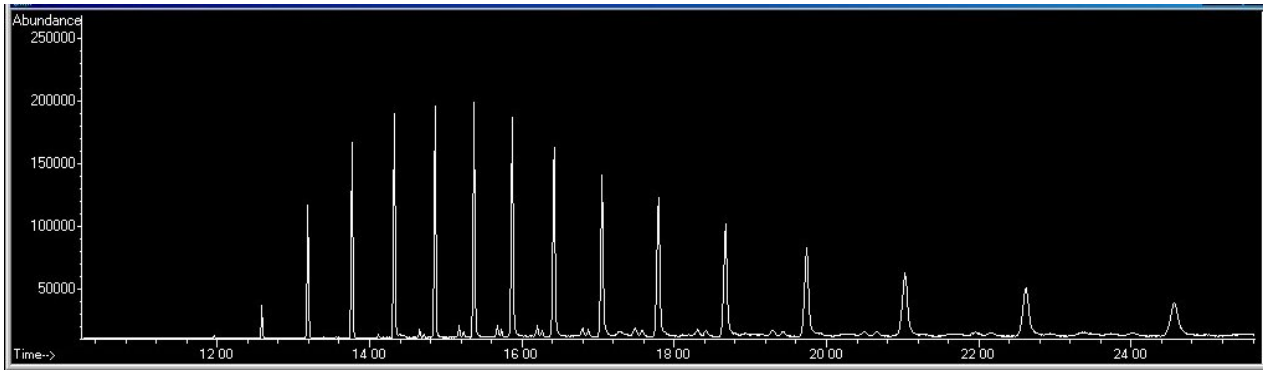

Figure 5. Chromatographic analysis of the commercial paraffin wax. Based on this result, it was decided [10] to select docosane, C_{22}, as a pure hydrocarbon analogous to the wax.

3.1 Wax

The commercial wax was a Sigma-Aldrich Chemicals product designated MP 73-80 DEG (cat no. 411671-1, CASRN 110-82-7). Analytical grade cyclohexane was obtained from Riedel-deHaen and anhydrous 99 % octane from Aldrich Chemicals*.

The stock solvent was a mix of 25 ml of octane and 25 ml of cyclohexane. A potentially wax-precipitating mixture was prepared by adding a given amount of the wax to the stock at 75°C and stirring until the mixture was clear. Three mixtures were prepared for the majority of the experiments labeled by the ratio corresponding to the mass (in grams) of wax added to 50 ml of solvent, namely 3:1, 1:1 and 0.25:1 (or 1:4). [For example, a designation 3:1 indicates that 150 g of wax were mixed with the 50 ml of solvent.]

3.2 n-Docosane

Docosane [CH_3 $(CH_2)_{20}CH_3$ purity > 98 %, MP 42-45°C] was obtained from Fluka Chemicals. A 1:4 mixture was prepared at 45°C for the experiments reported here.

3.3 Visual Observations

Initially, we carried out straightforward independent visual observations on the mixtures as they were cooled. The objective was to get a crude estimate of the gel point of the wax systems, defined loosely as the temperature below which the mixture could not easily be poured from the container. The qualitative visual properties of the mixtures were as reported below.

3.3.1 Wax mixtures

a) 3:1 mixture;

The mixture was opaque above 65°C and formed a hard homogeneous gel at about 38°C. Thus, the gel point is approximately 38°C.

……

*Trade names are given in this paper so that the experiments could be repeated if necessary. Endorsement by NIST or ANSTO is not implied.

b) 1:1 mixture;
Cloudiness was seen at 72°C and the mixture became opaque at ~ 70°C. The mixture became white and viscous as the temperature dropped. At about 54 °C there was a marked increase in viscosity, while at ~38°C the mixture was such that it could not be poured from the container for several hours. Thus, the gel point is designated at ~ 38°C.

c) 1:4 mixture;
Cloudiness was seen at 57°C, and a gel point was observed at about 28°C. The gel was soft but homogeneous.

3.3.2 Docosane

The mixture was cooled from the initial 45°C while stirring. Small crystals were first seen at ~19°C and were distributed evenly through the solution. When the same cooling experiment was performed under static a condition that is in the absence of stirring large needle-like crystals grow against the container walls. In the context here, we thus observed that the docosane mixture cooled to a floc, in contrast to the wax samples which formed a gel.

4.0 Instrumentation

4.1 Neutron scattering: SANS

In order to perform neutron scattering experiments on these samples it was necessary to work with deuterated solvents to provide scattering contrast between the wax and the solvent. The wax was mixed in various concentrations with a solvent made up of deuterated cyclohexane (Sigma-Aldrich cat no.151866, CASRN 1735-17-7) and deuterated octane (Sigma-Aldrich cat no.151971, CASRN 17252-77-6). Samples were prepared with a wax/solvent ratio of 0.25:1 (1:4), 0.375:1, 0.5:1, 0.625:1, 0.75:1, 0.875:1 and 1:1. The samples were warmed to 75°C then loaded into preheated 0.1 cm thick, 2 cm diameter quartz neutron scattering cells using a warm syringe. The SANS component of the experiments was performed on the 30 m SANS NG7 spectrometer of the NIST Center for Neutron Research configured with an incident neutron wavelength λ = 5.0 Å (0.5 nm) and using sample-detector distances of 5.00 and 13.00 m. The instrument's 2D position-sensitive detector was offset by 0.20 m at the 5.00 m sample-to-detector distance to increase the accessible wave vector range $0.04 < q\ (\mathrm{nm}^{-1}) < 1.45$. Here, the wave vector $q = (4\pi/\lambda) \sin(\theta/2)$, where θ is the angle between the incident and scattered neutron beams.

Loaded scattering cells were placed in the Center for Neutron Research's thermostatted 10-cell sample changer, in which the temperature of a given cell was recorded by a thermocouple placed in the sample block. A calibration correction provided by the Center for Neutron Research for the difference between the actual cell temperature and the block temperature was subsequently applied. The samples were taken to an initial temperature of 80°C and equilibrated at that temperature for 1 hour. For a given sample, the scattered intensity, I, was then recorded. The temperature was then reduced sequentially by 5°C intervals and the intensities remeasured after temperature equilibration times of 30 minutes, Following this scheme, data were taken in 5° C temperature decrements between 80 and 10°C. (In some cases, 80 and 20°C.)

In order to test if 30 minutes was sufficient for equilibration and to test for any possible hysteresis effect, the intensity measurement of a given sample was repeated at the

end of a complete sample run over all temperatures. This corresponded to an additional equilibration time of approximately one hour. No noticeable difference was detected in the scattering patterns from a given sample at a given temperature at the beginning and at the end of the data acquisition.

Since all measured scattering patterns were isotropic, the intensity data were azimuthally averaged. Corrections to the intensity were made for empty cell and solvent scattering, and the corrected data were placed on an absolute scale by normalizing to the absolute neutron flux as measured with a calibrated, intensity-reducing absorber placed in the beam. No other corrections were applied.

4.2 Dynamic Light scattering

Dynamic light scattering was performed on an ALV compact goniometer (ALV, Germany) with ALV 5000E correlator card. Samples were prepared in 10 mm diameter cylindrical scattering cells and placed in a toluene index-matching bath. Temperature control was achieved using a circulating water bath, with an accuracy of ±0.1°C. The samples were illuminated with a HeNe laser (λ = 633 nm), and all measurements reported here were carried out at a scattering angle of 40° (wax) and 90° (n-docosane). Measurements were either of 30 s or 60 s duration, and the results shown are the averages of a minimum of three repeat measurements.

4.3 Rheometry

Rheological measurements were performed with a commercial stress-controlled Haake CS-150 rheometer connected to a Haake DC5-K75 water circulator that controlled a temperature range between 5° and 75°C with an accuracy of ± 0.3°C. A double cone, DC60/2^{o} closed geometry system was used to prevent volatilization to ensure a consistent shear rate in the total volume of the solution. All measurements were at ambient pressure conditions.

All tests were carried out using freshly prepared samples as described in Section 3. Once dissolved at 75°C (paraffin wax) or 45°C (docosane), the samples were loaded into the rheometer preheated to 75°C and 45°C respectively. They were then subjected to an applied shear, with shear rates ranging from 0.5 s^{-1} to 1500 s^{-1}. At a given shear, rate the samples were cooled down slowly over either 5 or 10 hours to about 10°C, and the shear stress was recorded as a function of time, i.e., as a function of temperature.

In some cases, a separate study of the viscometric properties was performed using a rheometer configured in the cone and plate geometry. The lower plate was thermostatted to 25°C by water circulating in an integrated compressor cooling circuit, and the sample temperature was monitored using a platinum resistance element. A solvent trap minimized evaporation from the mixture during these measurements.

5.0 Results and discussion

5.1 SANS data

5.1.1 Wax mixtures

Representative SANS intensity patterns as a function of the wave vector, q, are displayed in Figures 6 and 7. Figure 6 illustrates how the intensity changes as a function of temperature for mixture 1:1 (see section 3), while Figure 7 gives the corresponding data from

the more dilute sample, 1:4. Results from the two detector settings are shown and, as expected, are consistent (the shift at the lowest temperature in Figure 7 is an insignificant apparatus artifact).

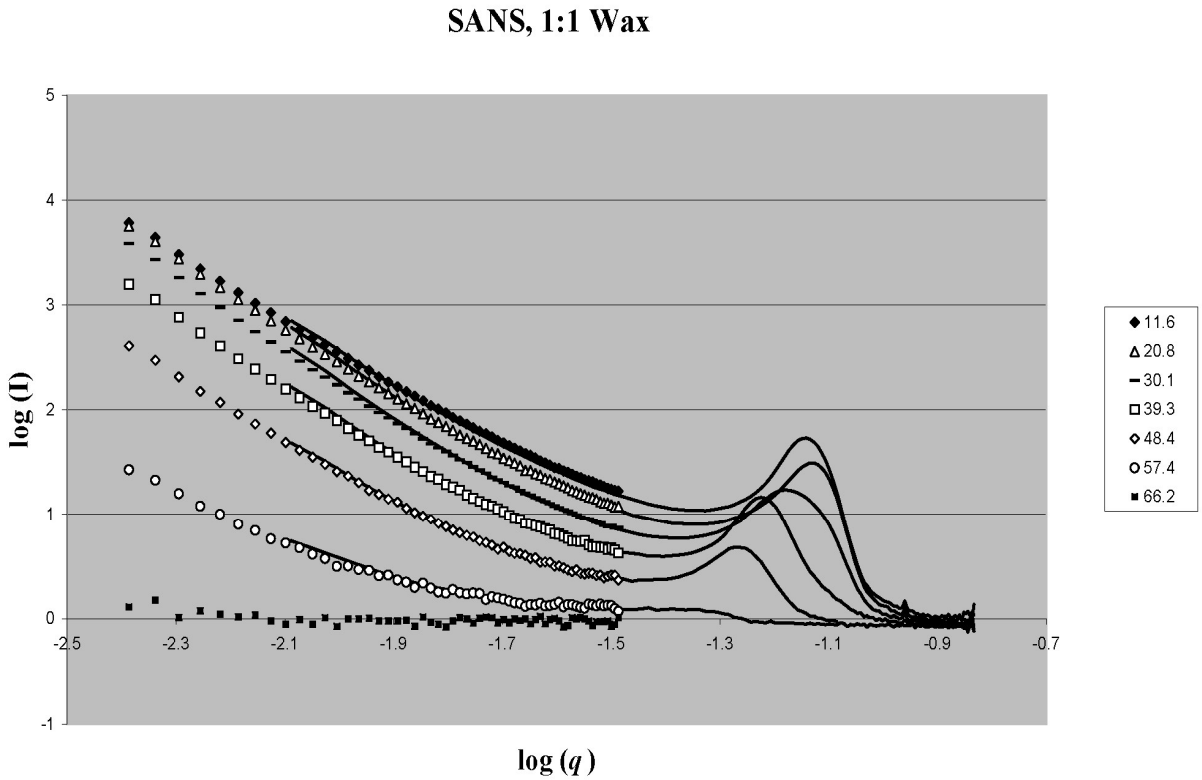

Figure 6. Logarithmic plot of the SANS intensity (I, cm^{-1}) versus the wave vector (q, $Å^{-1}$) as a function of temperature for the wax mixture designated 1:1, see section 4.1. Data taken at a detector setting of 5 m are given by the lines. Symbols denote data taken at 13 m. The temperatures, °C, are noted in the box. Note that an above background signal is apparent at 57.4 °C. At lower temperatures, an intensity peak is apparent at the higher values of q.

Despite the concentration difference, the two sets of curves are similar. The signal above background is obvious even in the higher temperatures and a definite maximum in the intensity curve is observed at $q \sim 0.05$ $Å^{-1}$, which corresponds to a characteristic length in the system of about 125 Å (12.5 nm). As the temperature falls, the maximum becomes a well-defined peak which moves to a higher wave vector with declining temperature.

5.1.2 Docosane

The SANS data patterns taken with docosane differed significantly from those of the wax in that no significant signal was observed until the temperature had dropped to 20°C; and then only for the more concentrated sample 1:1. Even at 20°C the two sets displayed completely different features which are clearly shown from the 2-dimensional detector images, Figures 8 and 9. Figure 8 displays the intensity from the wax sample at the two detector settings, 5 m and 13 m. The radially symmetric intensity ring pattern at the higher wave vectors is strikingly obvious, as is the smooth rise in intensity at lower q. Compare the corresponding images from docosane in Figure 9. Nothing is detected above background for the 0.25:1 (1:4) mixture. Anisotropy at low q is detected from the 1:1 sample, but there is a complete absence of structure at higher q.

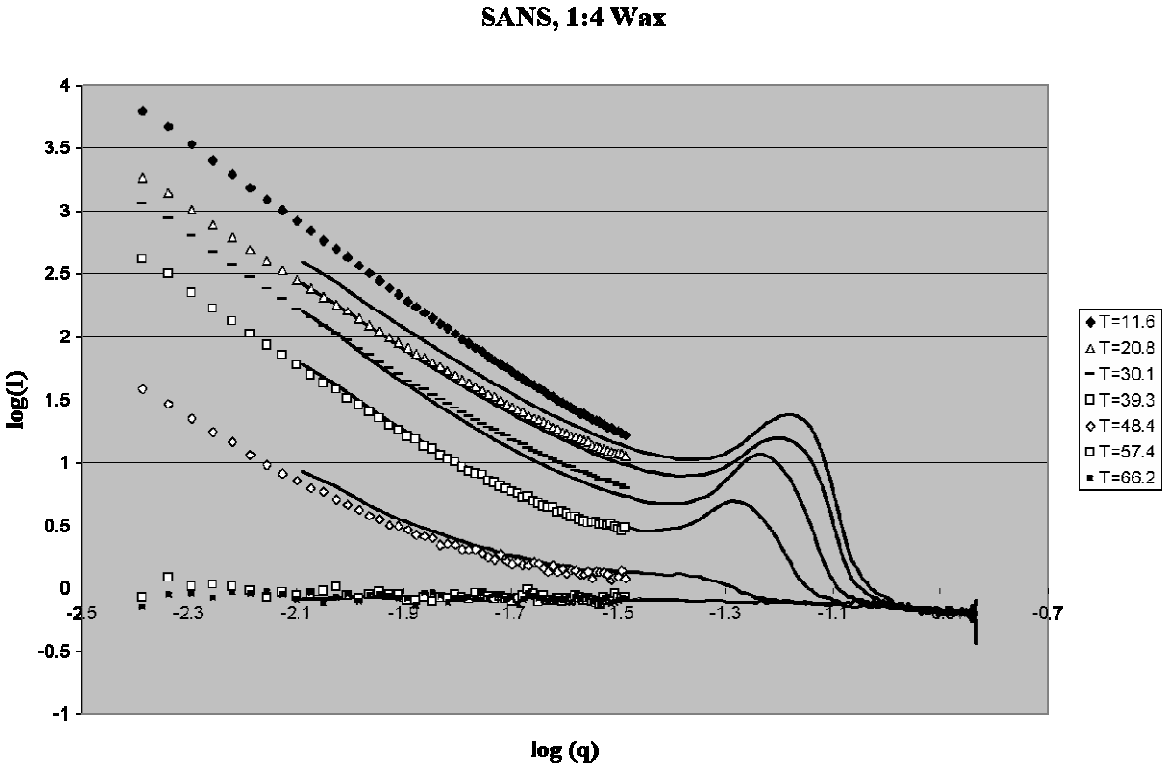

Figure 7. Logarithmic plot of the SANS intensity (I, cm^{-1}) versus the wave vector (q, A^{-1}) as a function of temperature for the wax mixture designated 1:4. Data taken at a detector setting of 5 m are given by the lines. Symbols denote data taken at 13 m. The temperatures, °C, are noted in the box. The overall pattern of these curves tracks that observed for the more concentrated mixture, see Figure 6.

5.2 DLS data

5.2.1 Wax, 1:4 Sample

The majority of experiments were carried out with the 1:4 sample. We noted that this sample remained transparent down to 40°C, at which point it started to become slightly turbid. Measurements could be made down to about 30°C before multiple scattering became too large. The apparent hydrodynamic radius of the wax sample, corrected for the temperature dependence of the solvent viscosity, is shown in Figure 10 as a function of temperature. In all cases the data could be fit with a monomodal distribution centered on the value shown, with no evidence of larger structures. There was however considerable variation and this is reflected in the size of the error bars. The structures measured using dynamic light scattering are in all cases of the order of micrometers, in contrast to the SANS results which showed structures on the order of 10 nm. However, as light scattering intensity is proportional to the square of the radius, structures of the order of 10 nm scatter ten thousand times less than structures of the order of micrometers. Thus the DLS results show that large scale structures are present, but do not preclude the existence of the 10 nm structures.

We are confident that the differences between SANS and DLS are not due to experimental uncertainties. A straightforward speculation is that the smaller nanoscale structure exists inside a larger more nebulous microstructure. One is tempted to assume that the nanoscale length scale corresponds to a fractal object. A fractal object, however, would

be expected to grow in size as the temperature falls. While the scattered intensity does indeed increase with decreasing temperature, the position of the high-q peak maximum should move to lower q if this reasoning is correct. This is not the general trend.

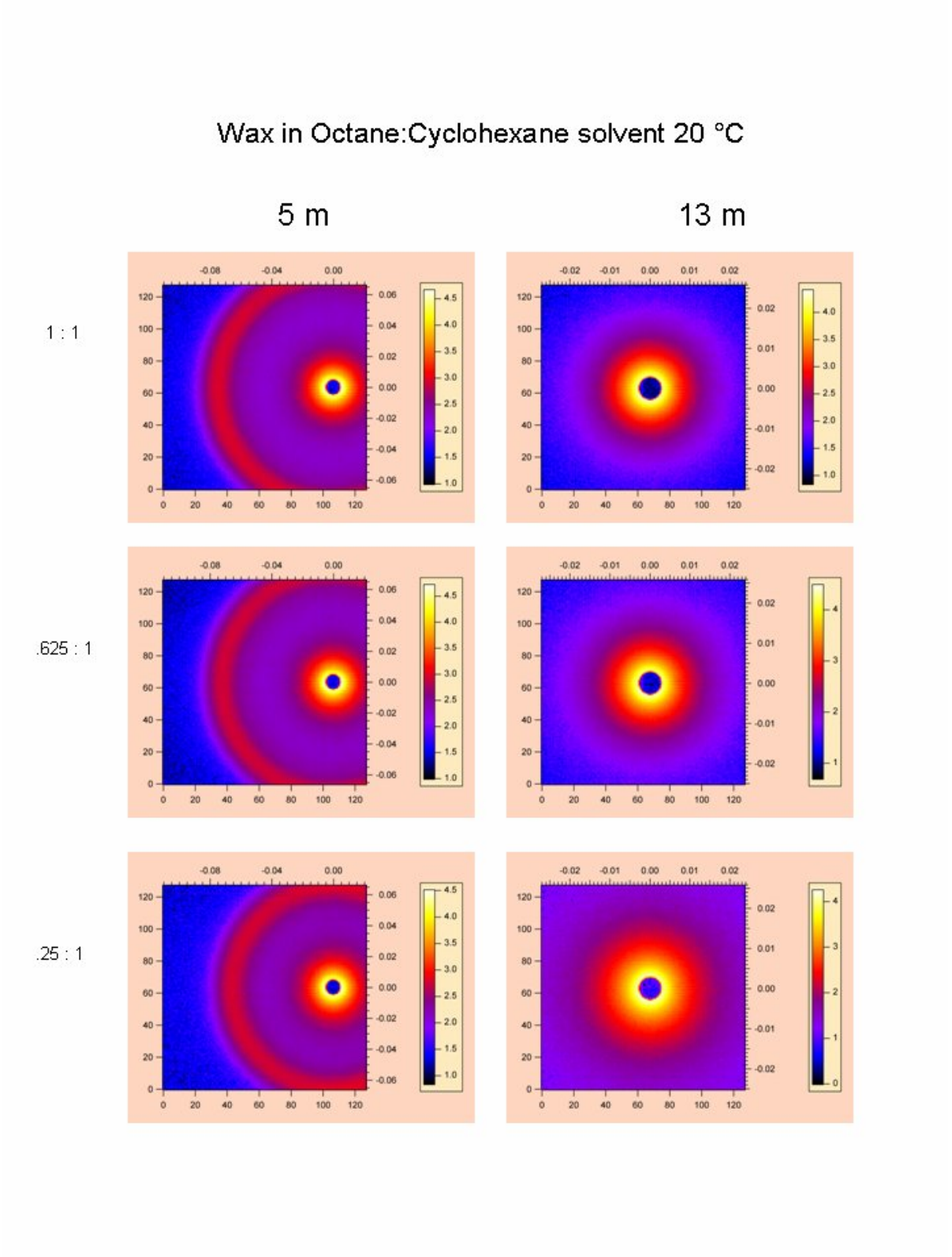

Figure 8. Raw 2-dimensional SANS detector images from wax samples. Note the obvious features indicating an intensity maximum at higher values of q, and a definite intensity slope at lower q. Azimuthally averaging gave curves corresponding to Figures 6 and 7.

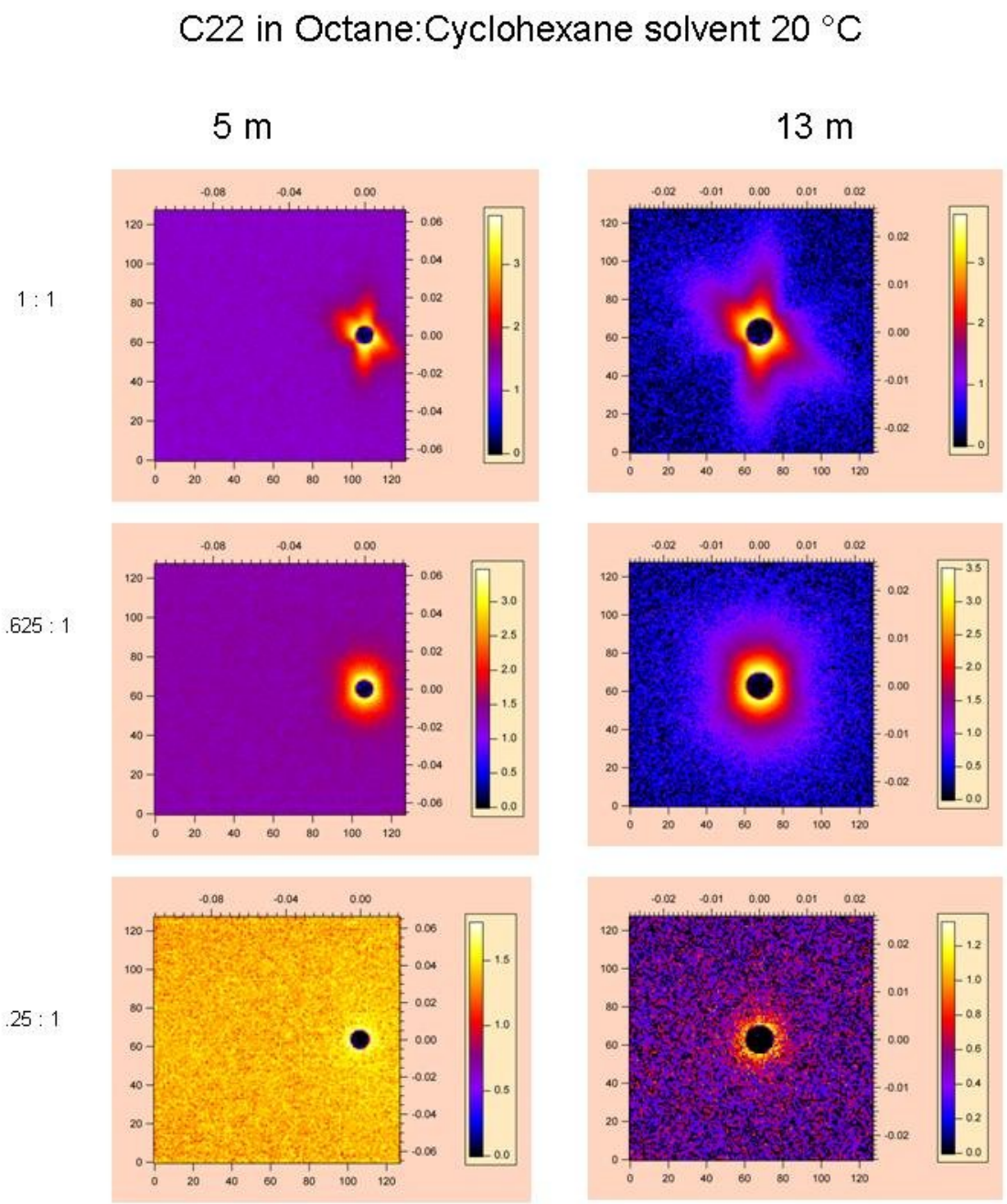

Figure 9. Raw 2-dimensional SANS detector images for the 1:1 sample from docosane samples. Compare with Figure 8. Note the anisotropy at low q values - characteristic of a crystal - but also note the complete absence of any ring structure.

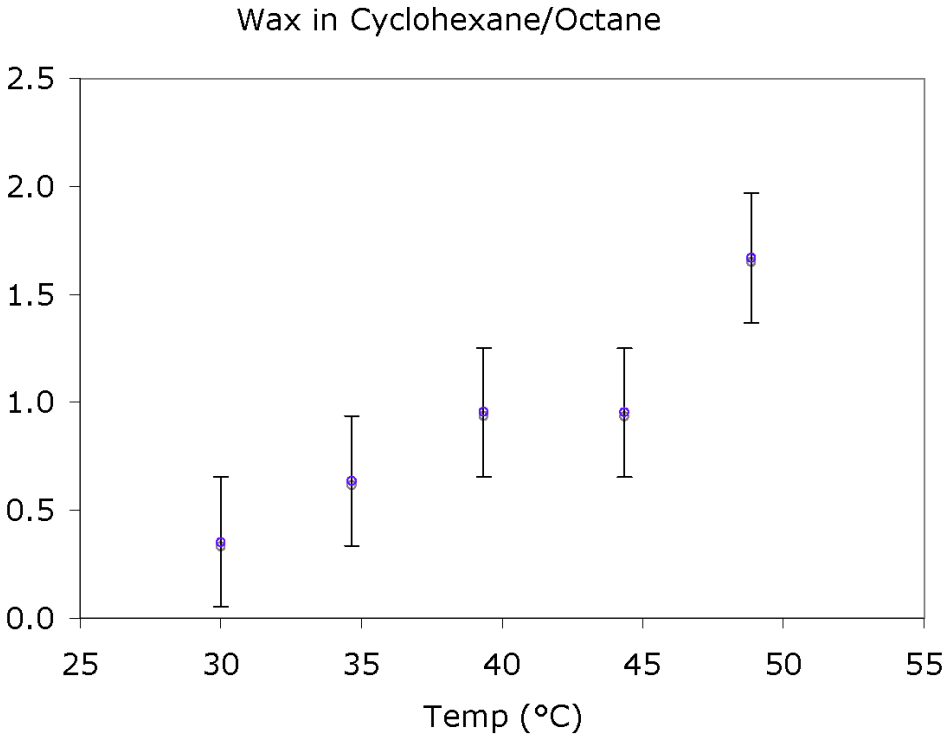

Figure 10. Apparent hydrodynamic radius (μm) of the 1:4 wax sample as a function of temperature. The radius has been corrected for the temperature dependence of the solvent viscosity. Cooling was carried out over 90 minutes. Measurements could not be made below 30°C. There was a large degree of variability in the measurements. Time dependence of gelation was not investigated in this measurement.

5.2.2 Docosane

Figure 11 displays the variation of the autocorrelation functions (ACFs) observed from the C_{22} sample over the temperature range 45°C down to 15°C. The functions show no systematic variation between 45°C and 20°C. In each case there are two clear decays – a fast decay which is approximately the same for all samples, and a slow decay which changes character at 15°C. The fast decay corresponds to a (number weighted) apparent radius of about 200 nm which remains unchanged down to 13°C (Figure 12). The slow decay represents partially restricted motion, which may be due to some very large particles or agglomerates.

Figure 12 shows measurements between 15°C and 10°C. While there is a demonstrable change in the ACF between 15°C and 13°C, there is a dramatic change between 12°C and 10°C. At 10°C the sample is clearly in the gel state – where there is no fast decay. In this state, at 10 °C, there is no motion in the sample observable with DLS over a timescale of at least hundreds of seconds.

The ACF in this case shows a very long time decay. However, this is likely to be an artifact of the measurement – in order to measure these accurately, non-ergodic averaging methods would need to be employed [12]. In addition, at both 12°C and 10°C the samples are no longer transparent, so multiple scattering also contributes to the results.

However, the results show unequivocally that there is precipitation between 1°C and 10°C. Re-warming the sample to 15°C gives an ACF very similar to that prior to cooling (Figure 12). The transition is therefore reversible, even after repeated cooling and warming cycles. The results also show that the C_{22} behaves very differently from the commercial wax.

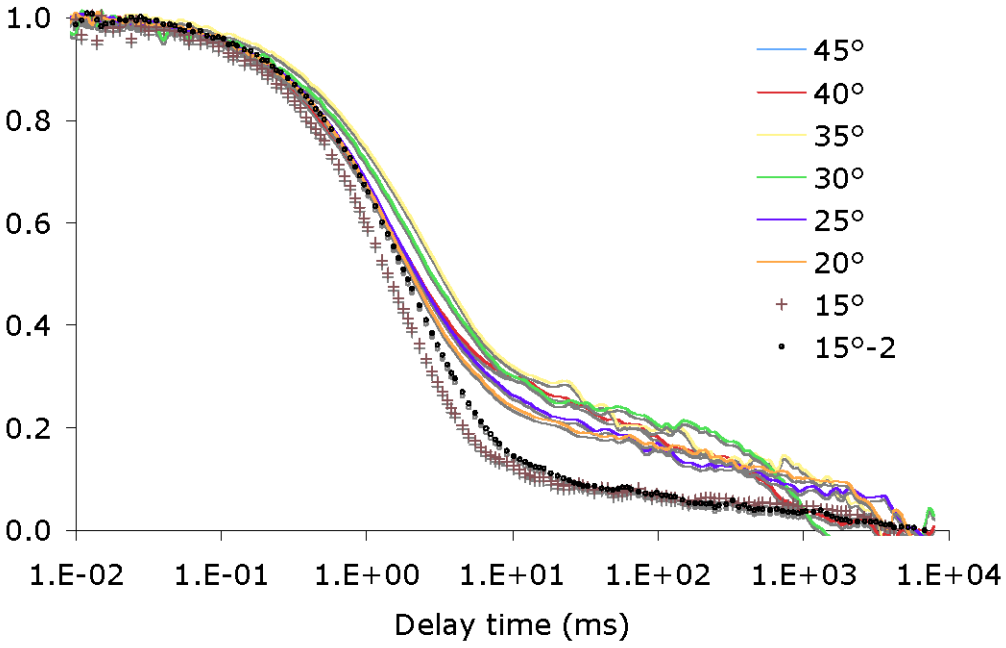

Figure 11. Autocorrelation functions of n-docosane as functions of decreasing temperature from 45°C to 15°C. Cooling was carried out over 90 minutes. No significant change is apparent down to 20°C. There is a change in the character at 15°C. The second run at 15°C was taken after 18 hours equilibration, and showed no significant change.

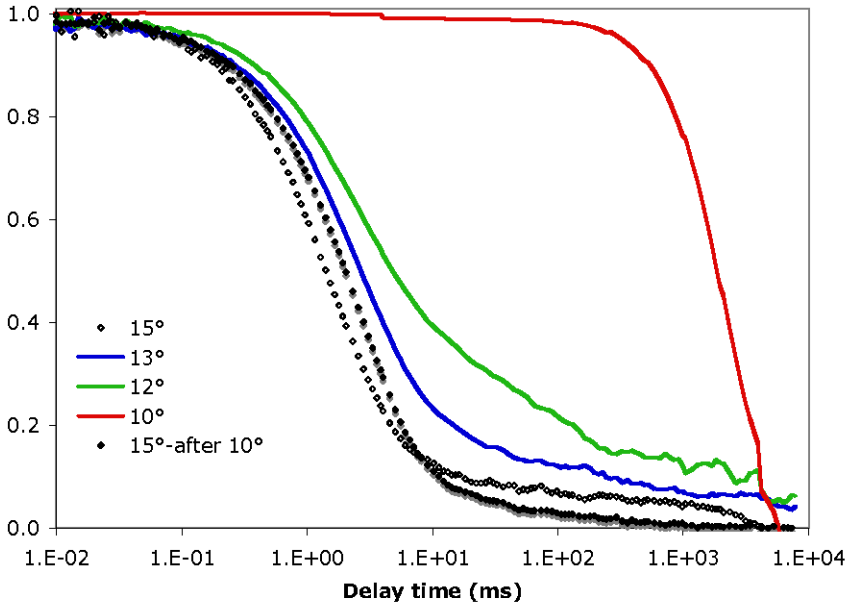

Figure 12. Autocorrelation functions of n-docosane at temperatures in the range 10-15°C. The first measurement at 15°C was carried out after 18 hours equilibration – no significant change was observed in this time. The sample was then cooled in one degree increments and left to equilibrate for 5 minutes at each temperature before each measurement. Following cooling to 10°C, the sample was returned to 15°C for the final measurement.

5. 3 Rheometry

5.3. 1 Solvent viscosity

Figure 13 depicts the experimental viscosity (η) of the cyclohexane/octane solvent. The viscosity set was fitted to the simple equation: η (Pa·s) = $(-6.0 \cdot 10^{-6}) \cdot T + 0.00076$, with the temperature, T, in °C, valid over the limited temperature range studied here. The data are consistent with independent measurements of other authors [13]. [As matter of interest; we include a prediction from the NIST transport prediction routine, SuperTrapp [14]. SuperTrapp overestimates the experimental values by about 8 %, but this discrepancy is not considered significant in the context of this investigation: it is known that SuperTrapp can slightly overestimate the viscosity of cyclic-hydrocarbons without a special correction.]

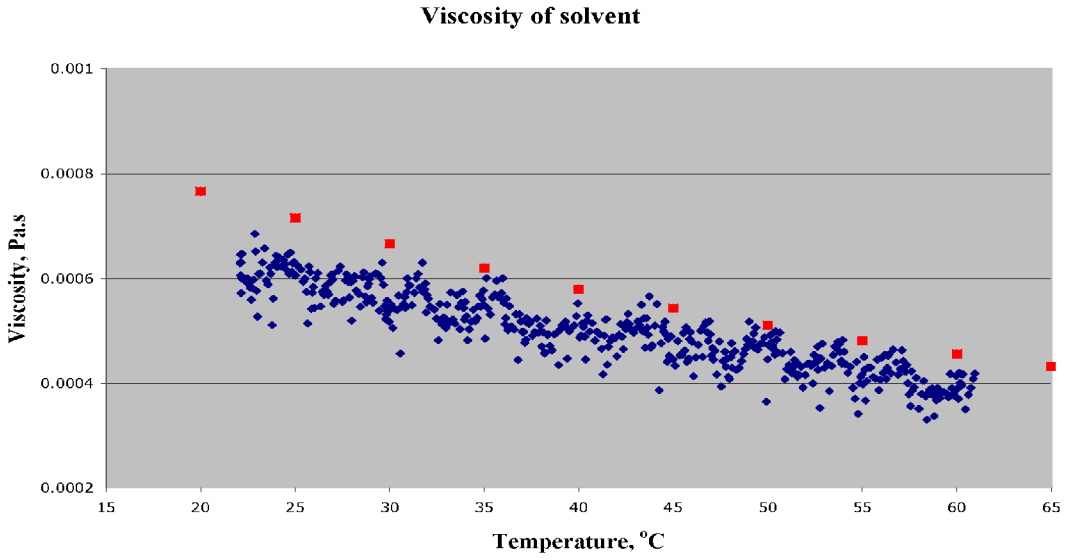

Figure 13. Data (diamonds) for the viscosity of the solvent – a 50 % mixture of cyclohexane and n-octane (see Section 3.1) – over the temperature range considered in this work. The squares are calculated values from NIST routine SuperTrapp. Despite the systematic deviation, the agreement is considered satisfactory.

5. 3. 2 Wax, Systems 3:1, and 1:1

Figure 14 presents a plot of the 3:1 wax mixture subjected to a shear rate of 1 s^{-1} as a function of decreasing temperature (time) measured over a 10 hour period. A 3:1 mixture is unrealistic in the sense that a real crude oil would not have such a high wax concentration, but the curve exaggerates a general trend observed when all wax mixtures are cooled. We see that the viscosity increases strongly as the temperature falls, far exceeding the temperature dependence of the solvent alone (Figure 13), even at relatively high temperatures. But, at a temperature close to that which we loosely designate a gel point (in this case about 38°C) the viscosity plateaus and then declines. The graph is notable in that the qualitative trend is very similar to that observed from rheological studies of a gelling colloidal silica suspension [7], as we first pointed out in Section 2, above. And see the Appendix. The result gave us confidence in thinking of wax deposition as a gelling process.

The trend – the sharp viscosity (or stress) increase as wax deposition accelerates – is made more noticeable if the temperature is fixed at slightly below the gel point. Figure 15a displays the stress-temperature plot for a 1:1 mixture subjected to a shear rate of 500 s^{-1} when the temperature is held constant at 31°C and the system allowed to gel at this temperature for several hours. It shows that in this experiment, even after several hours, we may still be in a transient regime. Also shown is Figure 15b, for which the constant temperature was set only one degree higher, 32°C. Both experiments report the same general variation of the stress with temperature, but the results may indicate how sensitive the numerical value of the stress, or the viscosity, is to a slight change in the temperature.

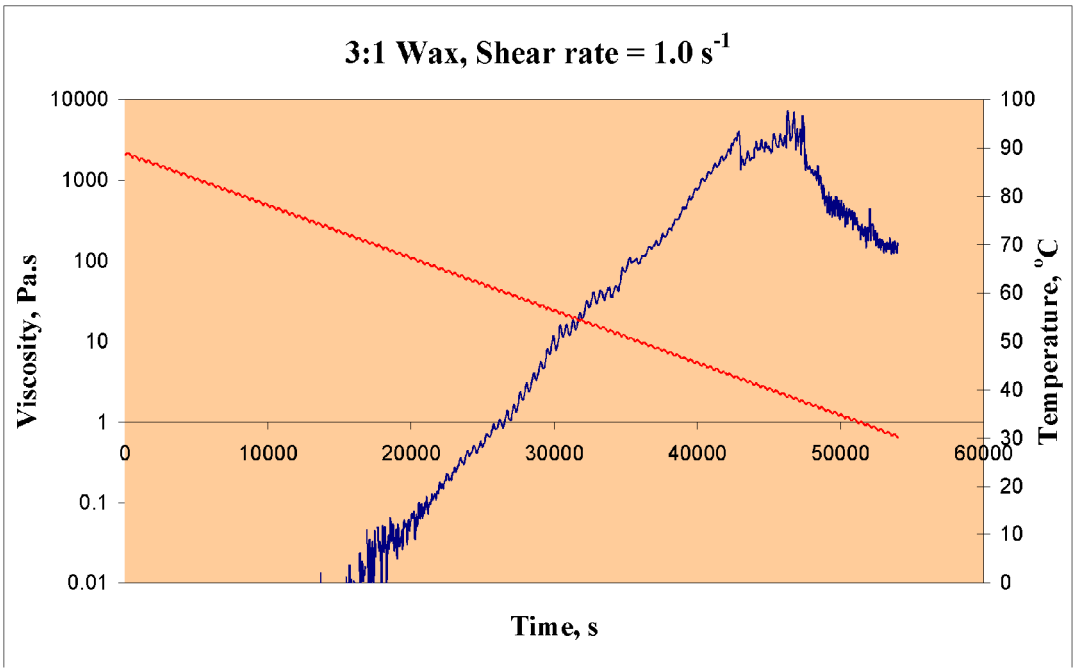

Figure 14. Plot of the viscosity versus temperature (time) for a 3:1 wax system subjected to a shear rate of 1 s^{-1}. Blue curve, viscosity: red line, temperature. Note that the viscosity increases strongly, plateaus, and then declines. The parallels with the behavior of colloidal silica gelling under shear are discussed in the text. See the Appendix.

5.3.3 Wax, System 1:4

The majority of shearing runs were performed on the 1:4 wax samples for which a body of data was recorded over a grid of initial configurations, applied shear rates, cooling rates and other experimental variables. Representative results are presented. For example, Figure 16 shows a stress curve at the low applied shear of 0.5 s^{-1}. At such a low shear rate the effect of shear is minimal, but the small hump at about 55°C is definite and reproducible. It is unclear what this implies, but equates with the SANS results which indicate that a structural change takes place in the wax at around this temperature.

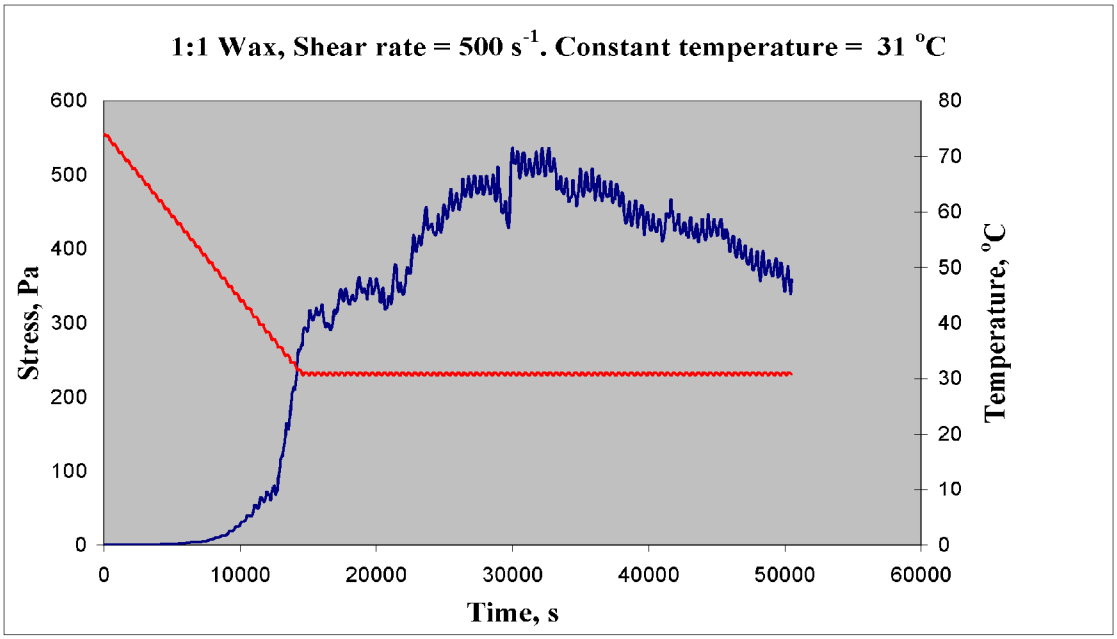

Figure 15a. Stress-temperature plot for the 1:1 wax system subjected to a shear rate of 500 s^{-1}. Blue curve, stress: red line, temperature. The temperature was held constant at 31°C and the system allowed to gel for several hours.

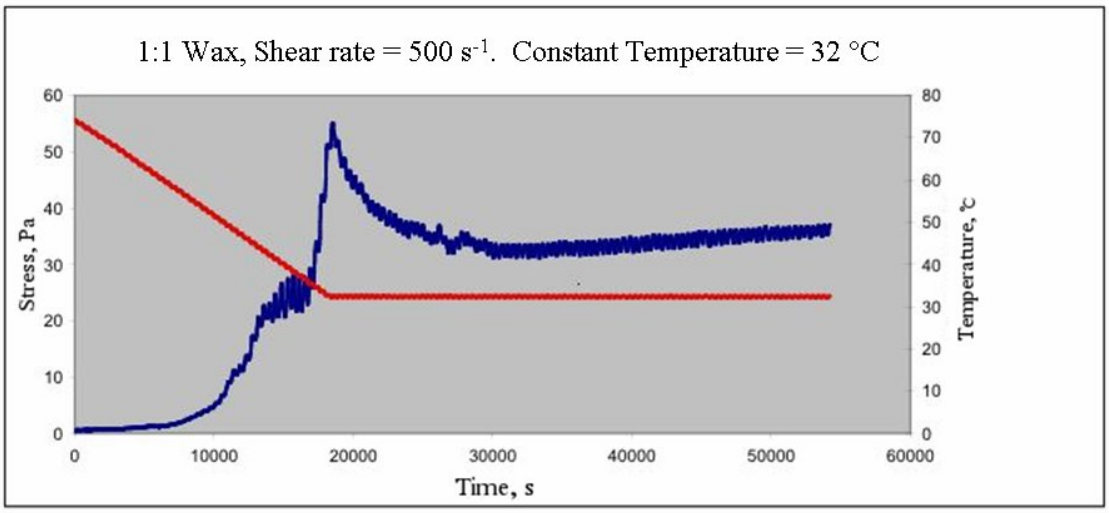

Figure 15b. Stress-temperature plot for the 1:1 system subjected to a shear rate of 500 s^{-1}. Blue curve, stress: red line, temperature. The temperature was held constant at 32°C and the system allowed to gel for several hours. The behavior during the initial five hour cooling period is similar to that shown in Figure 15a, but note how much a small change on the assigned constant temperature can alter the quantitative result.

Figure 17 compares the stress variation with temperature corresponding to applied shear rates (s^{-1}) of 0.5 (lower curve, as in Figure 16), 500 (middle), and 1500 (upper). The data at low temperatures for the 500 s^{-1} run do not follow the other two curves, but the general trend is clear: all curves, even the run at the lowest shear rate, indicate a local maximum stress at around the 28°C gel point.

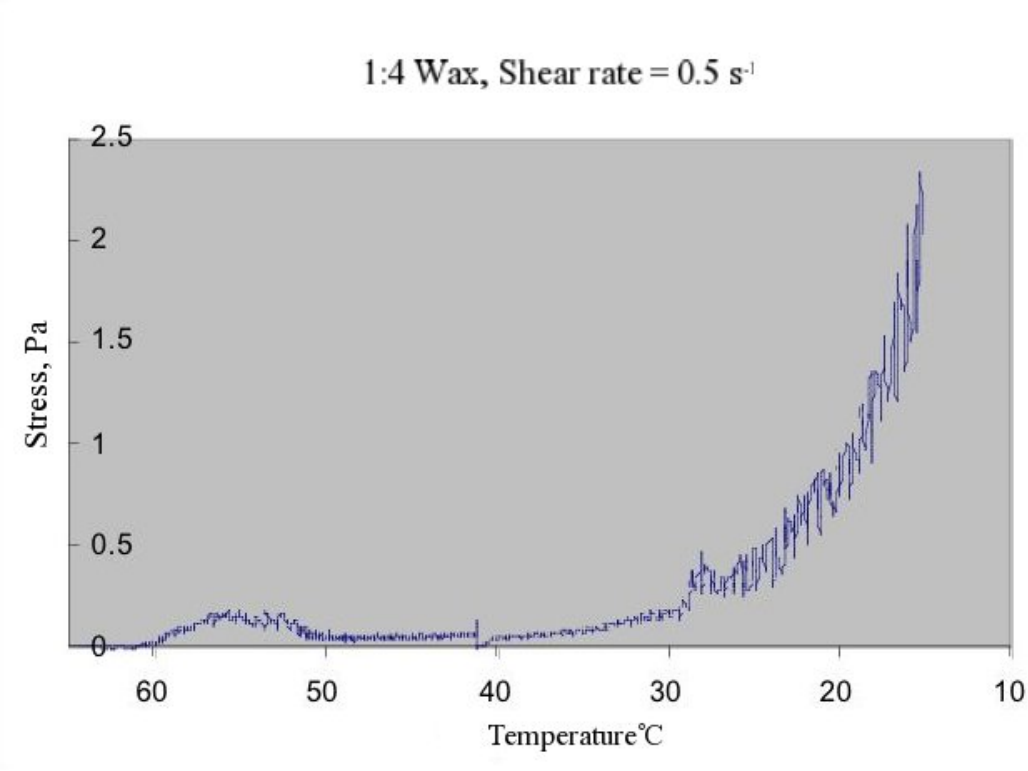

Figure 16. Stress vs. temperature curve from the 1:4 wax system subjected to a shear of 0.5 s^{-1}. Note the definite maximum at about 55°C.

5.3.4 Comparison. 1:4 systems with C_{22} and wax

Figure 18 illustrates how 1:4 mixtures with C_{22} and wax, respectively compare when subjected to the low shear rate 0.5 s^{-1}. The wax curve is close to exponential (Figure 16) over the temperature range displayed, whereas the C_{22} curve increases and exhibits large variations below about 20°C. This merely reflects that the C_{22} becomes crystalline. Of more interest is Figure 19 that compares the samples when both are subjected to a shear rate of 1500 s^{-1}. From this plot one can conclude that the wax is able to withstand a stress: it is a gel. Whereas, the C_{22} is a floc and the high imposed shear breaks it up.

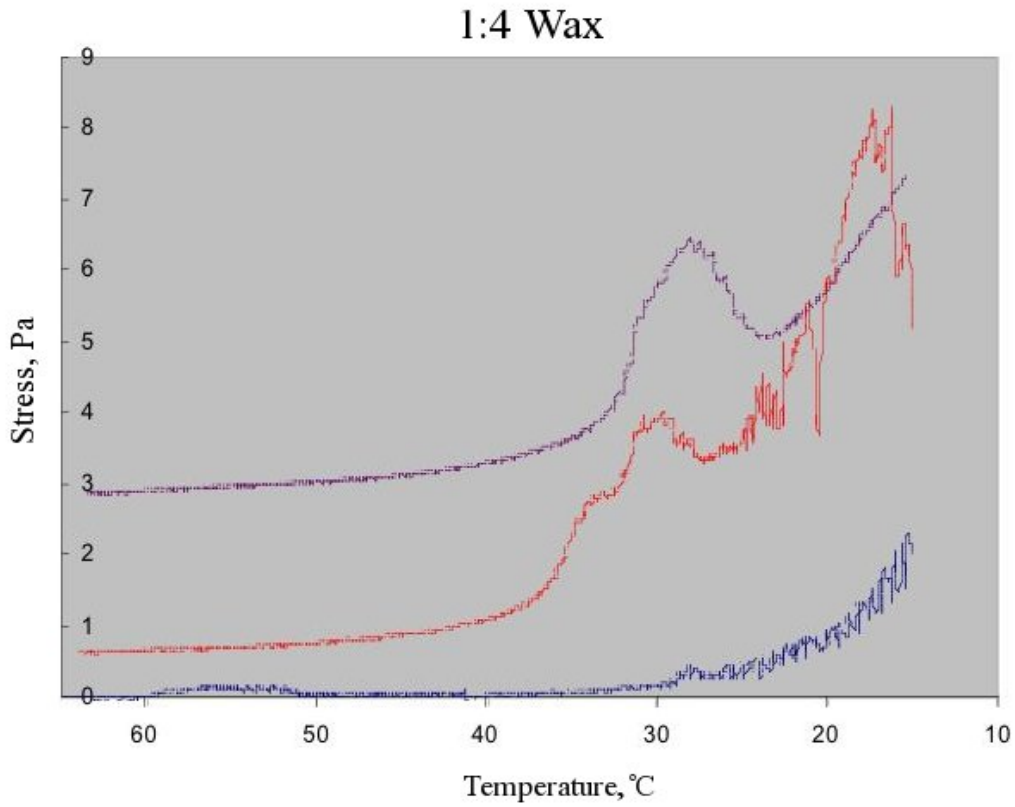

Figure 17. Stress - temperature curves from the 1:4 wax mixture subjected to shear rates (s^{-1}) of 0.5 (lower curve), 500 (middle), and 1500 (upper). Compare with Figure 14 representing a much more concentrated system.

To conclude: we have demonstrated that out initial premise that wax formation should be treated as a gelation process is justified. We have demonstrated a strong connection between the structure of waxy gel and its rheological behavior. The work, however, has raised a number of questions that will have to be answered from further work. In particular there is an apparent discrepancy between the conclusions that would follow from the SANS and DLS data, as mentioned in section 5.2.1. Further, it is necessary to carry out a simultaneous SANS/rheology experiment in order to equate precisely the rheological behavior with the wax nanostructure: this is planned for the near future.

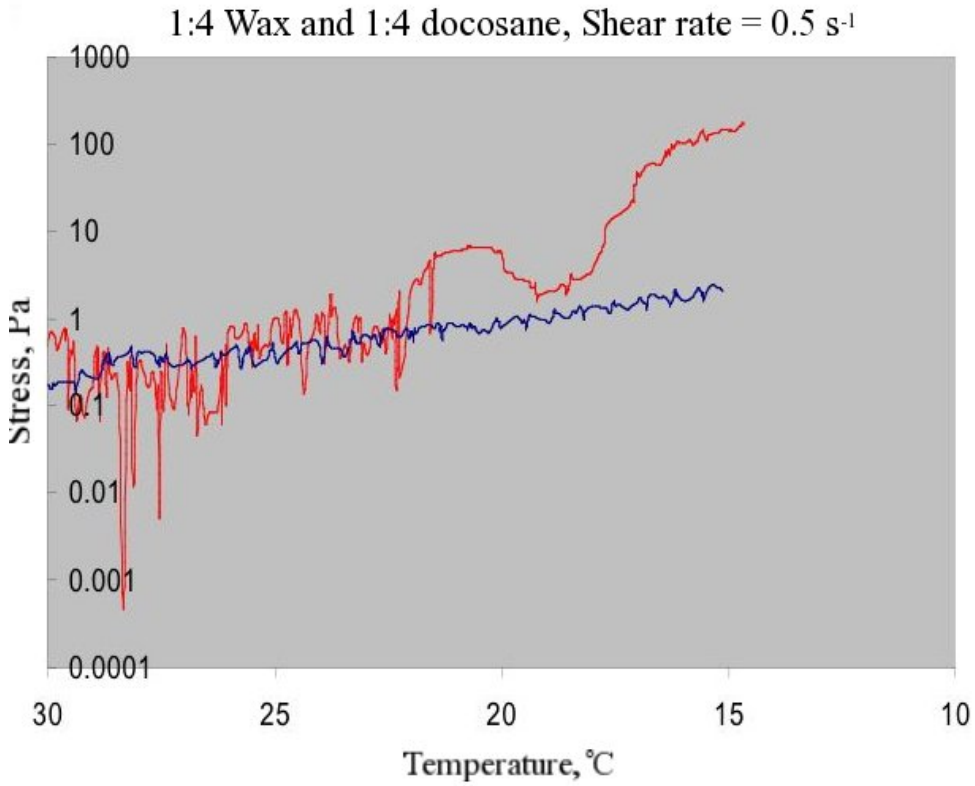

Figure 18. Lower temperature range comparison of the 1:4 wax stress variation with temperature (smoother curve) with that of docosane C_{22}. Shear rate, 0.5 s^{-1}.

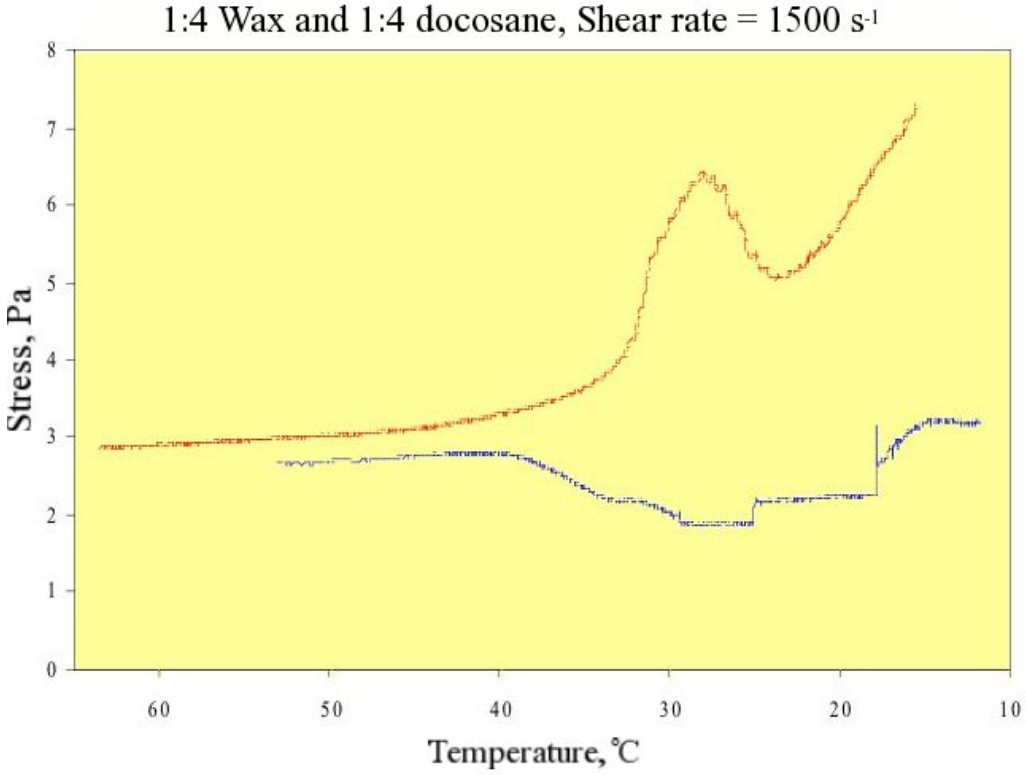

Figure 19. Comparison of the wax stress (upper curve) with that of C_{22} (lower curve) when the systems are subjected to an applied shear rate of 1500 s^{-1}.

References

[1]. Oil production and the efficiency of existing or new wells must be as optimal as is economically feasible, especially since industry must now exploit ever deeper reservoirs, heavier crudes, and off-shore sites. Even ten years ago the Australian Petroleum Resource Book [P. McGregor, *The Australian Petroleum Resource Book*, AIP (Melbourne, 1996)] contains the comment:

> Unfortunately, even the combined finds *(of oil deposits*) of recent years cannot replace the bonanza of Bass Strait, which is now declining in influence. We are now faced with two choices, one leads to dependence on fuel from overseas. The other offers an opportunity to find more Australian oil.

Similar sentiments were expressed in a report from Woodside [*Woodside Australian Energy, ABARE Outlook, 2002*]. To quote:

• Projections by Australian Government forecasting agencies indicate that Australia is facing a rapid decline in liquid petroleum production over the next decade. Liquids self-sufficiency is expected to decline from an average of 80-90 % over the past decade to less than 40 % by 2010.
• The economic implications for Australia are significant including a rapid deterioration in Australia's trade deficit on liquid hydrocarbons (from a surplus of $1.2 billion in 2000/01 to a projected deficit of $7.6 billion by 2009/10).
• Declining production over the next decade appears inevitable. However, options to reduce the longer-term decline are available. These will take time to implement so urgent action is required.

[2]. Flow assurance is a standard topic of petroleum research. Major facilities in Australia include the Woodside Research Facility at Curtin University, WA; Department of Engineering, University of WA; and the CSIRO Division of Petroleum Resources.
See A. Mansouri for many papers on this topic. Website:
http://tigger.uic.edu/~mansoori/Asphaltene.Deposition.and.Its.Control_html.
We are most grateful to Drs. Bob Hurle and Terry Edwards of the University of Western Australia, and Dr. Rob Trengove of Murdock University for extensive discussions on flow assurance in general and wax formation in particular. Figures 1, 2 and 4 were provided by Dr. Hurle.

[3] For example see: H.P. Ronningsen, B. Bjorndal, A. B. Hansen, and W. B. Pedersen, Energy Fuels **5,** 895-908 (1991).

[4] Convincing experimental evidence that the premise is valid first came from the papers of Beysens which reported shear influenced shifts in the critical point of simple fluids and mixtures. The issue was addressed directly by Hanley and Evans in their work on the computer simulation of model fluid, and by Romig and Hanley who showed that shear could change phase behavior radically.
D. Beysens, Physica **118A** 250 -267 (1983)
H.J.M Hanley, and D.J. Evans, J. Chem. Phys., **76,** 3225-3232 (1982).
K.D. Romig, and H.J.M. Hanley, Int. J. Thermophys., **7**, 877-885 (1986).

[5] M. Kahn, M. Djabourov and J-L Volle, Fuel **83**, 1591-1605 (2004).

[6] The petroleum literature does not address this premise directly, but it can be inferred from results reported by several authors. See especially [5] and the older work of Boger and coworkers: L.T. Wardhaugh and D.V. Boger, AICHE J **37,** 871 -85, (1991); L.T. Wardhaugh and D.V. Boger . Chem Eng Res Des. **67**, 74–83 (1987). Also see: I.V. Evdokimov, N Yu. Eliseev and D. Yu. Eliseev, J. petroluem Sci. and Eng. **30**, 199-211 (2001); J. A.Lopes da Silva and J. A.P. Coutinho, Rheo. Acta, **43**, 433-441 (2004); R.F.G. Visintin, R. Lapasin, E. Vignati , P. D'Antona and T. P. Lockhart, Langmuir **21**, 6240-6249 (2005).

[7] H. J.M. Hanley, C. D. Muzny, B.D. Butler, G.C. Straty, J. Bartlett and E. Drabarek, J. Phys.: Condens. Matter, **11,** 1369-1380 (1999).

[8] E. Drabarek, J.R. Bartlett , H.J.M. Hanley, J.L. Woolfrey, C.D. Muzny, and B.D. Butler, J. Sol Gel Sci. and Tech. 1**9**, 279-283.(2000).

[9] For a discussion on representing real crude by model systems see, for example: A.P. Radlinski and L. B Espinat, J. Molecular Structure **383,** 51-56 (1996).

[10] We are grateful to Dr. T. Bruno (NIST) for carrying out this analysis and for his suggestions as to the major components of the wax.

[11] For instance; H. Huanga, S. R. Larter, and G.D. Love, Organic Geochemistry **34**, 1673–1687 (2003); J. Poynter and G. Eglinton, Proceedings of the Ocean Drilling Program, Scientific Results **116,** 155-161, (1990).

[12] V. Martinez, G. Bryant and W. van Megen, Proceedings of the 17th National Congress of the AIP, paper 107, p. 1-4. ISBN 0-9598064-7-4. (2006).

[13] T.M. Aminabhavi, V.B. Patil, M.I. Aralaguppi and H.T.S.Phayde, J. Chem. Eng. Data **41**, 521 – 525 (1996).

[14] We thank Dr. Marcia Huber for discussions on the solvent viscosities. Calculations were made using the NIST prediction procedure: *NIST Standard Reference Database 4, NIST Thermophysical Properties of Hydrocarbon Mixtures Database (SuperTRAPP): Version 3.2*, Standard Reference Data, National Institute of Standards and Technology: Gaithersburg, VA, 2007.

Appendix. Gelling of colloidal silica under flow conditions and relevance to wax formation in crude oil.

We have argued that structural and rheological results from a gelling colloidal silica system are relevant to this study of wax formation. Some comparisons are outlined in this appendix.

A few years ago, SANS data indicated how an applied shear affects gelation by inducing changes in the gel structure [A1]. The system reported in Reference [A1] was an aqueous suspension of colloidal silica. We carried out a simultaneous *in-situ* SANS/rheology study of the effect of applied shear on the rheological properties of a gelling silica suspension, and on the structure of the network and clusters formed during the sol-gel transition. We found that, in the absence of shear, the viscosity of the system increases after gel initiation until it essentially goes to infinity at a time t_m which can be taken as the gelation time. As the system gelled under a constant shear rate, however, the viscosity at first increased as before, but then peaked at a time very close to t_m before decreasing monotonically to about 10 % of the maximum value (Figure A1). We noted that the viscosity maximum occurred when the stress reached a critical shear rate-independent threshold. The low viscosity state could be maintained apparently indefinitely by continuous application of shear, but the system gelled once the shear was removed.

The main conclusions of this study were:

1. Fluid flow retards gelation. Hence flow prevents network formation or - which is much the same thing - prevents the viscosity becoming infinite. The system, however, gels once flow ceases.
2. Contrary to what might be expected, the action of a shear does not break up clusters but rather densifies them and induces cluster growth.
3. The silica work shows that the properties and behavior of the system are fundamentally influenced by the action of an applied shear or stress.

In another investigation [A2], continuous oscillatory experiments indicated how shear controlled the structural evolution of the system during gelation (specifically, the evolution of the size and volume fraction of clusters and the extent of cluster-cluster cross-linking). In the absence of shear, we observed that the storage and loss moduli (G' and G'', respectively, initially increase slowly prior to gelation, indicating that cluster growth and network formation are initially proceeding slowly, but then the system evolves rapidly, with cluster growth occurring at a slightly faster rate than network formation. In contrast, sols pre-sheared for four hours prior to gelation exhibit rapid increase in both G' and G'' immediately after cessation of the applied shear (Figure A2), reflecting significant differences in the evolution of the gel structure. On ageing, the viscoelastic properties of the unsheared and pre-sheared samples are similar indicating that their structures are comparable on the length scales (several micrometers) being probed by the frequency range used in [A2]. However, their chemical and microstructural properties differ significantly, due to differences in the inter-cluster bonds. Thus, a gel formed after pre-shearing does not have the same structure as a gel formed in the absence of shear.

A further possible connection between our prior work on silica gels and wax gelation comes from a few observations reported in the petroleum literature.

When waxy crude is allowed to cool to the temperatures below the wax appearance temperature (WAT) a partial solidification of the high alkane paraffin occurs. The crystals agglomerate and are dispersed in the hydrocarbon solution. On further cooling, more crystals

appear and network to form a gel. It is also well known, however, that shear will retard this networking, see Figure 4 for example - hence the most obvious connection with the colloidal silica experiments. Further, we have reported in this work that the stress/viscosity -shear rate behavior of a sheared gelling wax system has a strong qualitative similarity with that of gelling silica: compare Figure A1 with the main text Figures 14, 15a and 15b. The observations from Kahn *et al.* [A3] are significant. To quote:

> The effect of the shear applied during cooling was systematically investigated by Wardhaugh and Boger, [A4]. The rheological properties for oil cooled at a given test temperature depend on shear rate, thermal history and time. For a fixed shear rate, after an increase of the shear stress during the cooling stage, with the temperature kept constant, the stress decreased and finally reached a constant value after several hours depending on the cooling rate.

Wardhaugh and Boger [A5] also observed that their sample could be left overnight after shearing, without any change of the flow properties, provided that the temperature does not change.

Conclusions reported by Kahn *et al.* are also revealing. Shown is a graph indicating their results for the shear moduli of wax gel forming after an initial shear, Figure A3. Compare Figure A3 from the wax with Figure A2 from the silica. Notice, for example, the rapid increase in the moduli with time at initial times.

[A1] H. J.M. Hanley, C. D. Muzny, B.D. Butler, G.C. Straty, J. Bartlett and E. Drabarek, J. Phys.: Condens. Matter **11**, 1369-1380 (1999).

[A2] E. Drabarek, J.R. Bartlett, H.J.M. Hanley, J.L. Woolfrey, C.D. Muzny, and B.D. Butler, J. Sol Gel Sci. and Tech. **19**, 279-283 (2000).

[A3] M. Kahn, M. Djabourov and J-L Volle, Fuel **83**, 1591-1605 (2004).

[A4] L.T. Wardhaugh and D.V. Boger, AICHE J. **37**, 871 -85, (1991).

[A5] L.T. Wardhaugh and D.V. Boger, Chem Eng. Res Des 1987; 67:74–83.

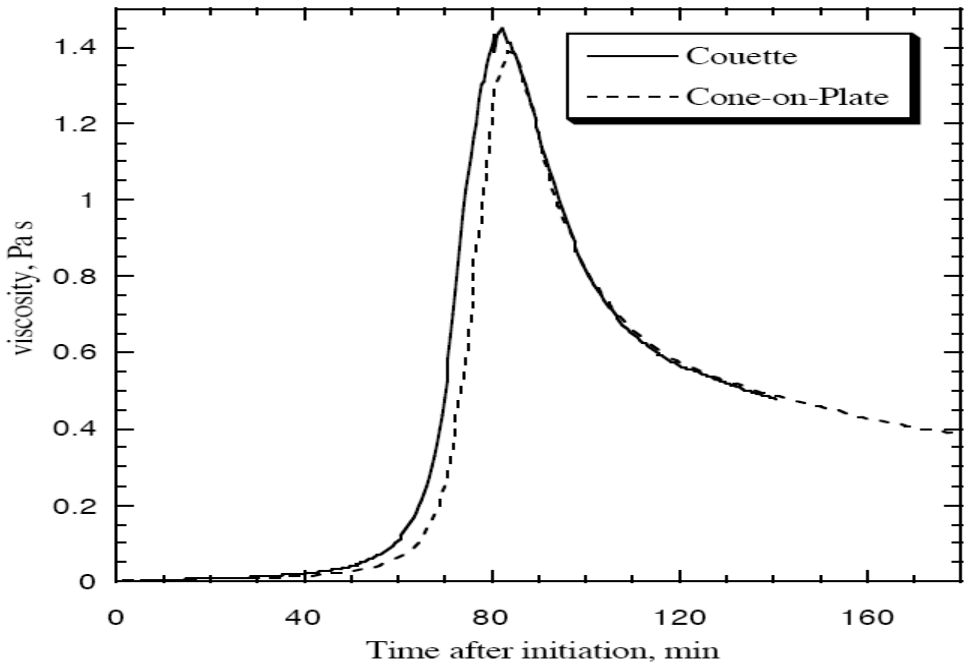

Figure A1. The viscosity of a gelling colloidal silica solution subjected to a shear as a function of time after gel initiation [A1]. The sol contained silica particles of 0.7 nm diameter at a volume fraction of 0.17. The applied shear rate was 250 s^{-1}. Results are given from a couette and a cone-on-plate rheometer.

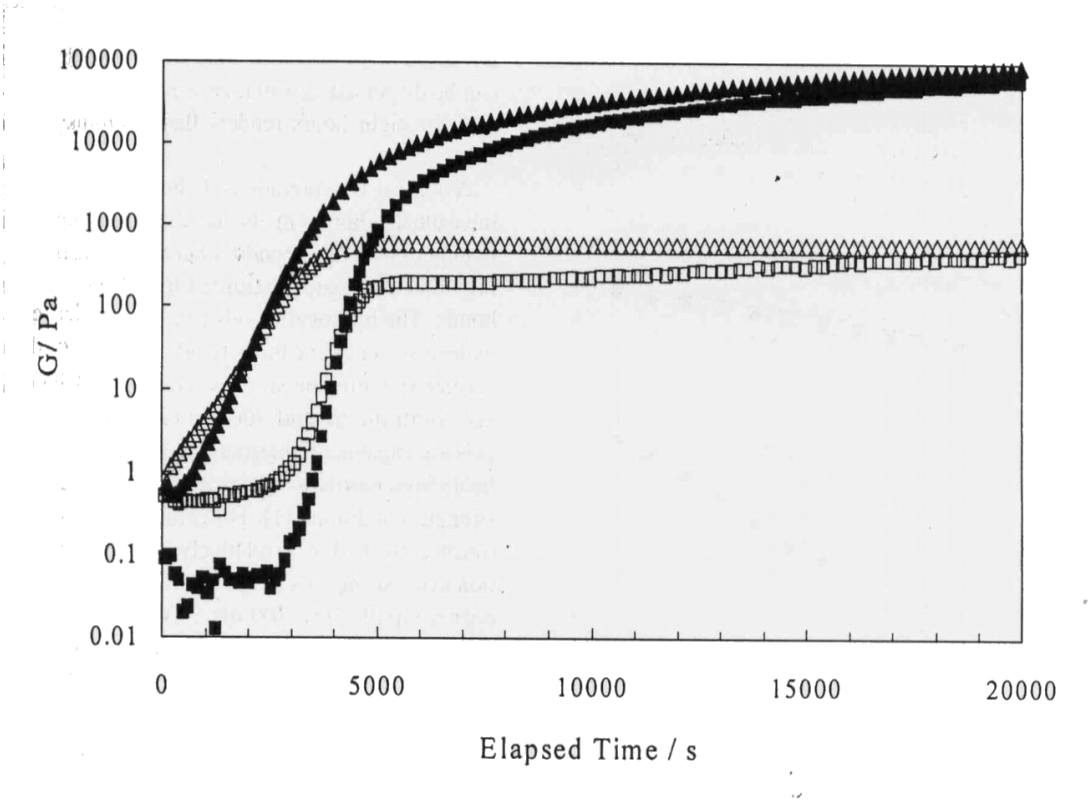

Figure A2. Variations in the storage and loss moduli, G″ and G′s, with time for the unsheared and presheared (at 500 s^{-1} for 4 hours) gelling silica sol. Solid squares, G′ (unsheared); open square, G″ unsheared); Solid triangles, G′ (presheared); open triangles, G″ (presheared). See Reference [A2].

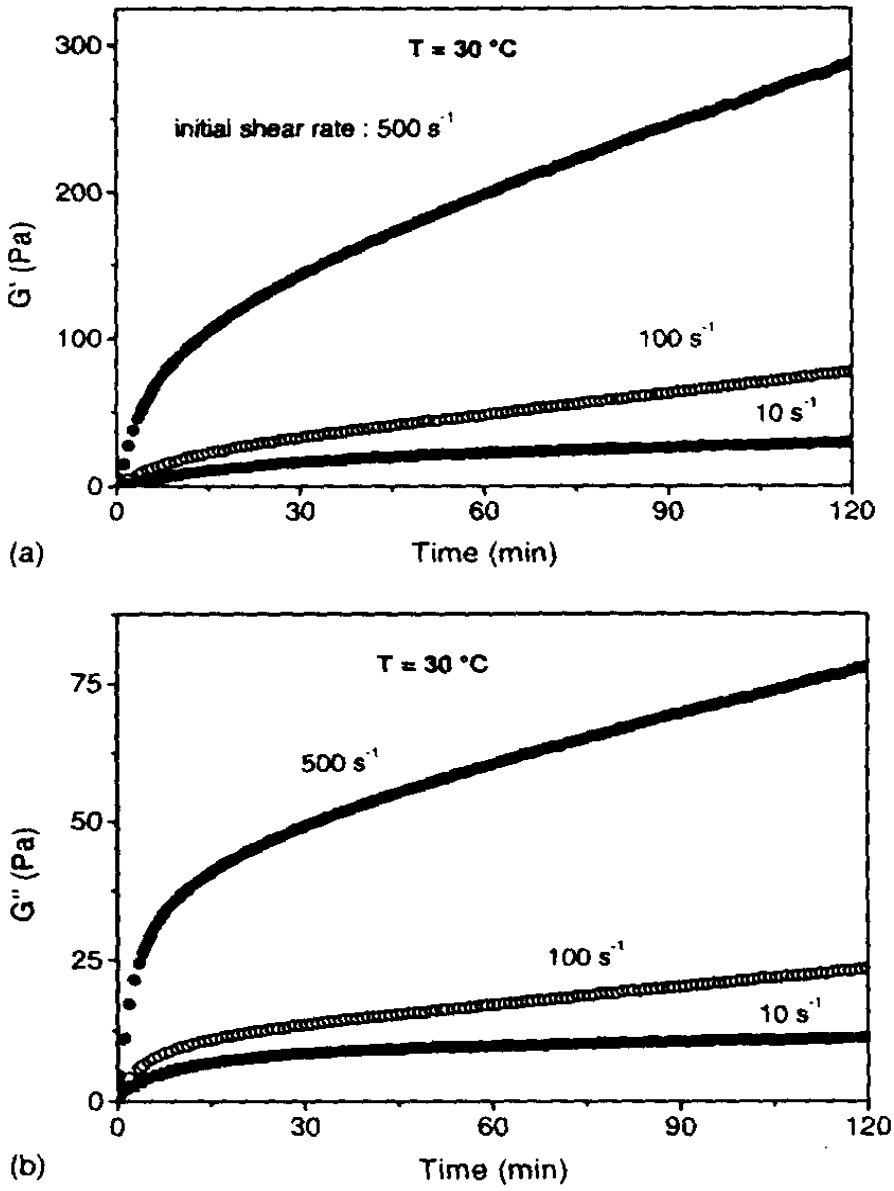

Figure A3. The variation of the storage moduli from a crude oil subjected to a shear [Data from Reference A3]. The comparison of their behavior with the corresponding behavior of gelling silica is striking, Figure A2. Note, in particular, the rapid increase in both G′ and G″ at very short times after shearing ceased.